Activity of TSC2 is inhibited by AKT-mediated phosphorylation and membrane partitioning

Sheng-Li Cai,[1] Andrew R. Tee,[2] John D. Short,[1] Judith M. Bergeron,[1] Jinhee Kim,[1] Jianjun Shen,[1] Ruifeng Guo,[1] Charles L. Johnson,[1] Kaoru Kiguchi,[1] and Cheryl Lyn Walker[1]

[1]Department of Carcinogenesis, University of Texas MD Anderson Cancer Center, Smithville, TX 78957
[2]Division of Molecular Physiology, University of Dundee, Medical Sciences Institute/Wellcome Building Complex, Dundee DD1 5EH, Scotland, UK

Loss of tuberin, the product of *TSC2* gene, increases mammalian target of rapamycin (mTOR) signaling, promoting cell growth and tumor development. However, in cells expressing tuberin, it is not known how repression of mTOR signaling is relieved to activate this pathway in response to growth factors and how hamartin participates in this process. We show that hamartin co-localizes with hypophosphorylated tuberin at the membrane, where tuberin exerts its GTPase-activating protein (GAP) activity to repress Rheb signaling. In response to growth signals, tuberin is phosphorylated by AKT and translocates to the cytosol, relieving Rheb repression. Phosphorylation of tuberin at serines 939 and 981 does not alter its intrinsic GAP activity toward Rheb but partitions tuberin to the cytosol, where it is bound by 14-3-3 proteins. Thus, tuberin bound by 14-3-3 in response to AKT phosphorylation is sequestered away from its membrane-bound activation partner (hamartin) and its target GTPase (Rheb) to relieve the growth inhibitory effects of this tumor suppressor.

Introduction

Tuberous sclerosis complex (TSC), caused by loss of function of either the *TSC1* or *-2* tumor suppressor genes, is an autosomal dominant disorder that leads to mental retardation, seizures, and the formation of tumors in various organs, including the brain, kidney, heart, and skin (Young and Povey, 1998; Gomez et al., 1999; Cheadle et al., 2000). The *TSC1* gene encodes the 130-kD protein hamartin (van Slegtenhorst et al., 1997), and the *TSC2* gene encodes the 198-kD protein tuberin (The European Chromosome 16 Tuberous Sclerosis Consortium, 1993). Hamartin contains two coiled-coil domains, which have been shown to mediate binding to tuberin (Hodges et al., 2001), forming a stable, functional tumor suppressor heterodimer within cells (Plank et al., 1998; van Slegtenhorst et al., 1998). Lesions that develop in TSC patients are histologically diverse; however, the tumors that arise as a result of loss of function of either TSC1 or -2 share common features, suggesting that hamartin and tuberin function within the same pathways to regulate cell cycle, cell growth, adhesion, and

vesicular trafficking (van Slegtenhorst et al., 1998; Hengstschlager et al., 2001). Recent studies have indicated that the hamartin–tuberin heterodimer regulates cell growth and proliferation as a downstream component of the phosphoinositide 3-kinase (PI3K)–protein kinase B (PKB/AKT) signaling pathway, which modulates signal transduction through target of rapamycin (TOR) in both *Drosophila melanogaster* and mammalian cells (Manning and Cantley, 2003; Inoki et al., 2005). Several distinct yet complementary genetic and biochemical studies collectively show that tuberin is a GTPase-activating protein (GAP) for the small GTPase Ras homologue enriched in brain (Rheb), which activates TOR and its downstream targets, such as the ribosomal S6 kinase (RSK; Li et al., 2004a).

Although loss of tuberin promotes cell growth and tumorigenesis, cells expressing tuberin must also be able to relieve tuberin repression of mammalian TOR (mTOR) signaling during conditions of mitogenic sufficiency. In this regard, tuberin contains multiple sites for AKT, MAPK, RSK, and extracellular signal–regulated kinase phosphorylation (Dan et al., 2002; Liu et al., 2002; Manning et al., 2002; Li et al., 2003; Tee et al., 2003; Roux et al., 2004; Ballif et al., 2005). Although it is clear that activation of AKT blocks tuberin inhibition of TOR signaling (Inoki et al., 2002; Manning et al., 2002; Potter et al., 2002), the mechanism by which

AKT inactivates this tumor suppressor is unknown (Bjornsti and Houghton, 2004). In addition, there are conflicting data regarding the subcellular localization of tuberin. For instance, independent studies report that tuberin can localize to the cytosol (Nellist et al., 1999), the membrane/particulate (100,000 *g*) fraction (Wienecke et al., 1995), and even the nucleus (Lou et al., 2001) of cells.

In this study, we sought to determine the mechanisms by which tuberin is regulated during cell growth. We found that tuberin is localized in membrane and cytosol fractions but not in nuclear fractions, and the translocation of tuberin from the membrane to cytosol is regulated by AKT signaling in response to growth factors. Phosphorylation of tuberin by AKT causes tuberin to become sequestered by 14-3-3 proteins in the cytosol. Mutation of two specific phosphorylation sites (S939 and S981) prevents the cytosolic translocation of tuberin from cellular membranes and results in a constitutively active protein that inhibits mTOR signaling. Importantly, tuberin phosphorylation by AKT does not affect its GAP activity toward Rheb in vitro but promotes Rheb-induced S6 kinase (S6K) 1 activation through increased Rheb-GTP loading in vivo. Therefore, it is likely that AKT phosphorylation inhibits tuberin as a result of 14-3-3 binding and cytosolic translocation rather than by impairing its catalytic GAP activity.

Results

Tuberin localization is regulated by Ser/Thr phosphorylation in response to growth factor stimulation

To investigate the subcellular localization of tuberin, mouse fibroblast (NIH3T3, Swiss3T3), rat kidney epithelial (TRKE2), human embryonic kidney (HEK293), and human breast cancer (MCF7) cell lines were fractionated, revealing that tuberin was detected within both the cytosolic and membrane fractions but not within the nuclear fraction (Fig. 1 A). Interestingly, tuberin in the membrane fraction migrated faster than tuberin within the cytosolic fraction (Fig. 1 A).

To determine whether this mobility shift was due to changes in phosphorylation, we treated these subcellular fractions with either a Ser/Thr or Tyr phosphatase (calf intestinal alkaline phosphatase [CIAP] or YOP protein tyrosine phosphatase, respectively). After CIAP treatment, the mobility of tuberin in the cytosol increased, resolving as a faster migrating band similar to tuberin purified from membrane fractions (Fig. 1 B). However, YOP did not affect tuberin mobility, indicating that the mobility shift was primarily due to phosphorylation of Ser/Thr residues. Treatment with CIAP resulted in both membrane and cytosolic tuberin migrating faster, indicating that tuberin within

Figure 1. **Tuberin localization is determined by Ser/Thr phosphorylation.** (A) Western analyses of subcellular fractions from the indicated cell lines using an anti-tuberin antibody. β1-integrin and lamin A/C proteins were analyzed as fractionation controls. Similar results were also observed with canine kidney cell lysates (not depicted). (B) Fractionated NIH3T3 lysates were treated with either CIAP serine/threonine phosphatase or YOP tyrosine phosphatase at 30°C for 1 h, and the electrophoretic mobility of tuberin was determined by Western analysis. (C) Swiss3T3 fibroblasts were serum starved (SV) for 24 h followed by serum stimulation (SM) with 20% FBS for the indicated times, and fractionated lysates were immunoblotted with the indicated antibodies. Phospho-AKT (S473) and phospho-AKT (T308) were blotted as controls for the effectiveness of the indicated treatments. Total lysates (top, M + C) were analyzed as controls for tuberin levels. Tuberin protein levels within the membrane and cytosolic fractions were determined as the percentage of total tuberin detected within both fractions. A representative blot from two independent biological replications is shown. Quantitation obtained from quintuplicate runs (*n* = 5) from each biological replicate is shown below. (asterisks) Both the reduction in the membrane fraction and increase in cytosolic fraction of tuberin that occurred in response to serum stimulation for 1 h were significantly different than starvation controls (*t* test, P < 0.02) and the 6 h time point (*t* test, P < 0.01). (D, top) Western analyses of tuberin from membrane and cytosolic fractions of serum-starved MCF7 cells (24 h) that were stimulated for 1 h with 30 ng/ml IGF-1 in the absence or presence of 100 nM of the PI3K inhibitor wortmannin. The vertical line indicates nonadjacent lanes in a single blot. (bottom) Tuberin protein levels within the membrane and cytosolic fractions were determined as the percentage of total tuberin detected within both fractions. A representative blot from three independent biological replications is shown. Quantitation is obtained from a total of seven independent Western blots from the three experiments. (asterisks) Both the reduction in the membrane fraction and increase in cytosolic fraction of tuberin that occurred in response to IGF-1 stimulation were significantly different from starvation controls (*t* test, P < 0.01) and the + wortmannin (*t* test, P < 0.01).
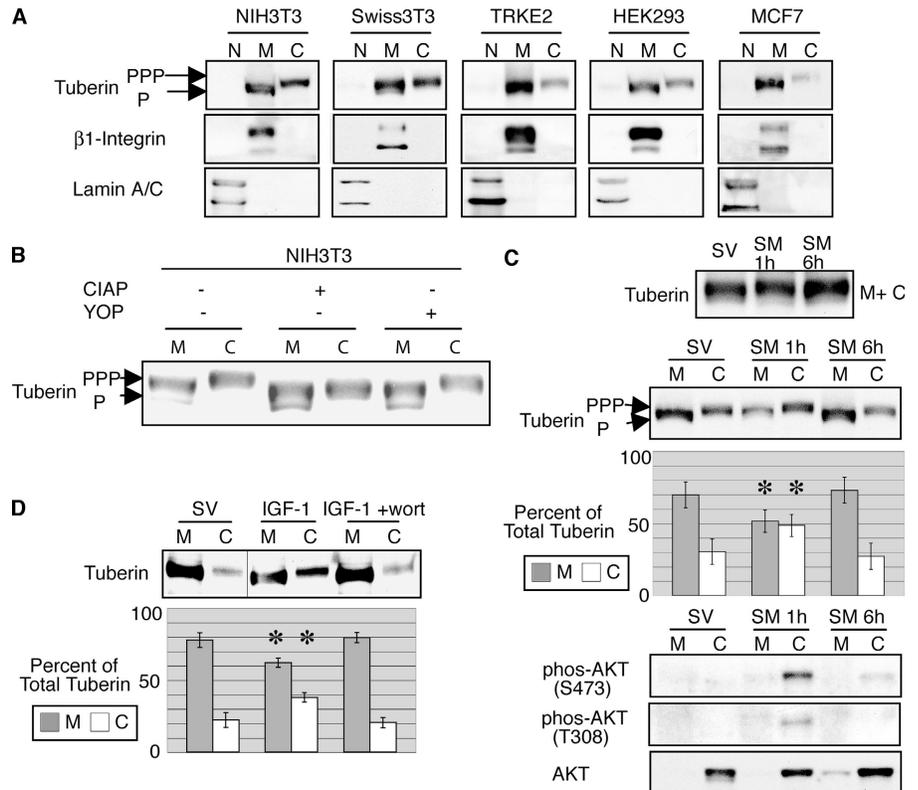
the cytosolic fraction is hyperphosphorylated. In addition, the serum-induced decrease in mobility of tuberin in both membrane and cytosolic fractions is likely driven by multiple phosphorylation events, as CIAP treatment (removing all Ser/Thr phosphorylation) increased the mobility of tuberin in both fractions.

To determine whether growth factor stimulation could also alter tuberin phosphorylation and subcellular localization, Swiss3T3 or MCF7 cells were serum starved and then stimulated with serum or insulin-like growth factor-1 (IGF-1) before fractionation (Fig. 1, C and D; and Fig. S1, available at http://www.jcb.org/cgi/content/full/jcb.200507119/DC1), as were NIH3T3 (Fig. S1 A) and TRKE2 cells (Fig. S1 B). Like serum, IGF-1 increased the amount of tuberin in the cytosolic fraction relative to starvation conditions (Fig. 1, C and D). In serum-stimulated cells, phosphorylation of membrane-localized tuberin was also increased after 1 h (comparable to cytosolic tuberin in starved cells but less than cytosolic tuberin from serum-stimulated cells; Fig. 1 C), suggesting that phosphorylation at specific residues, rather than total levels of phosphorylation, was determining localization. By 6 h, tuberin became predominantly membrane localized, which correlated with a decrease in AKT activation (Fig. 1 C). Translocation of tuberin from the membrane to the cytosol was blocked by the PI3K inhibitors wortmannin and LY294002 (Fig. 1 D and Fig. S1 B), implicating PI3K signaling in tuberin localization to the cytosol.

Tuberin translocation is mediated by AKT phosphorylation

To determine whether AKT directed tuberin's subcellular localization, tuberin from membrane and cytosolic compartments of NIH3T3 cells treated with IGF-1 or EGF was immunoprecipitated and detected with a (S/T) phosphosubstrate antibody that recognizes the consensus phosphorylation site for AKT and RSK containing phospho-Ser/Thr with Arg at position −5 and −3 (RXRXXpS/T) (Alessi et al., 1996; Obata et al., 2000; Yaffe et al., 2001; Roux et al., 2004). With equal tuberin loading (Fig. 2, A and B), the (S/T) phosphosubstrate antibody predominantly recognized tuberin within the cytosolic fraction, and the PI3K inhibitor wortmannin significantly reduced recognition of phosphorylated tuberin, suggesting that cytosolic tuberin was phosphorylated by AKT (Fig. 2, A and B). To confirm that activation of AKT directed tuberin to the cytosol, MCF7 cells stably transfected with a constitutively active AKT (myr-AKT) were examined and found to contain more cytosolic tuberin relative to wild-type MCF7 cells (Fig. 2 C). Recently, RSK was shown to phosphorylate tuberin at S1798 (Roux et al., 2004). To determine whether RSK phosphorylation of tuberin could regulate its localization, we generated a COOH-terminal deletion mutant of TSC2 at residue 1734 (referred to as Δ73) that lacks S1798 (Roux et al., 2004). Δ73 and wild-type tuberin had a similar distribution within membrane and cytosolic fractions under normal growth conditions (Fig. S1 C) and in response to serum (Fig. S2 A, available at http://www.jcb.org/cgi/content/full/jcb.200507119/DC1). In addition, overexpression of RSK1 did not affect localization of wild-type tuberin (Fig. S2 B). Collectively, these data indicate that tuberin residing in the cytosol is phosphorylated by AKT, suggesting that AKT (but not RSK) directly controls tuberin's localization and possibly its activity.

Mutation of AKT phosphorylation sites in tuberin alters its localization

Tuberin contains multiple S/T phosphorylation sites (Fig. 3 A). Among these, S1254 has been shown to be phosphorylated by MK2 (Li et al., 2003), whereas S939 (Inoki et al., 2002;
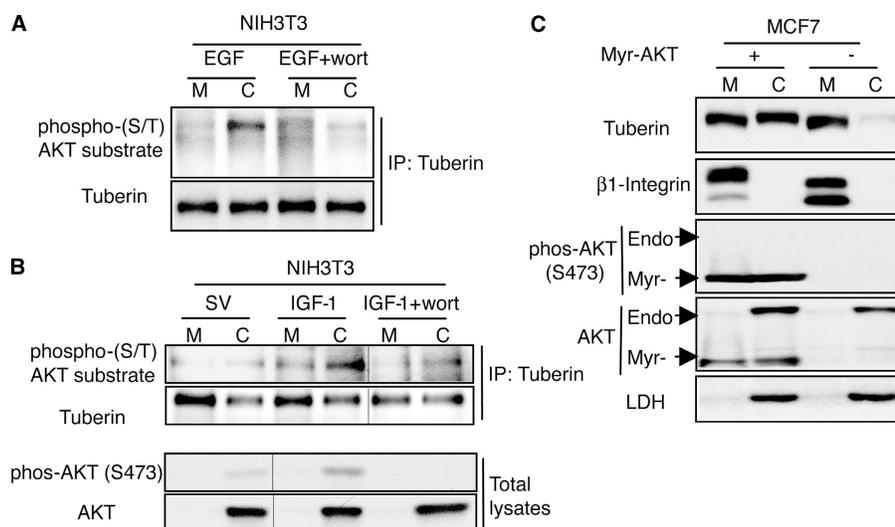

Figure 2. **AKT-mediated phosphorylation of tuberin leads to subcellular translocation.** (A) NIH3T3 cells were treated with 100 ng/ml EGF in the absence or presence of 200 nM wortmannin for 1 h. The fractionated cell lysates were immunoprecipitated with an anti-tuberin antibody (N19) followed by Western blot analysis with an anti–phospho-(S/T) AKT substrate antibody and an anti-tuberin antibody (C20). (B) NIH3T3 cells were serum starved for 24 h followed by treatment with 30 ng/ml IGF-1 in the absence or presence of 100 nM wortmannin for 1 h. The fractionated cell lysates were immunoprecipitated with an anti-tuberin antibody (N19) followed by Western blot analysis with an anti–phospho-(S/T) AKT substrate antibody and an anti-tuberin antibody (C20). Phospho-AKT (S473) was blotted as a control for the effectiveness of the indicated treatments. The vertical line indicates nonadjacent lanes in a single blot. (C) Western analyses of tuberin, AKT, and phospho-AKT (S473) were performed using membrane and cytosolic fractions from wild-type MCF7 and MCF7 cells that were stably transfected with constitutively active AKT (Myr-AKT). β1-integrin and LDH proteins were used as fractionation controls.

A

S939
S981
S1132   S1254 T1462
S1130   S1338   S1798
NH2 [GAP   ] COOH
                              1734 1807

Construct	WT		Mut
S939A:	RARST**S**LN	→	RARST**A**LN
S981A:	RCRSI**S**VS	→	RCRSI**A**VS
S1338A:	YSRSS**S**VS	→	YSRSS**A**VS
Δ73:	aa 1-1807	→	aa 1-1734
2A:	S939 + S981	→	S939A + S981A
S1254A:	LYKSL**S**VP	→	LYKSL**A**VP
S1130A/S1132A:			
	RDRVR**S**M**S**GG	→	RDRVR**A**M**A**GG

B

Transfect: Flag-TSC2   WT   SATA   T1462A   S939A   S981A   2A
                       M C   M C   M C   M C   M C   M C

Flag-Tuberin

hamartin

Rheb

β1-integrin

LDH

C

Transfect: Flag-TSC2   WT   2A   S1254A   WT   2A   S1130A/S1132A
                       M C   M C   M C   M C   M C   M C
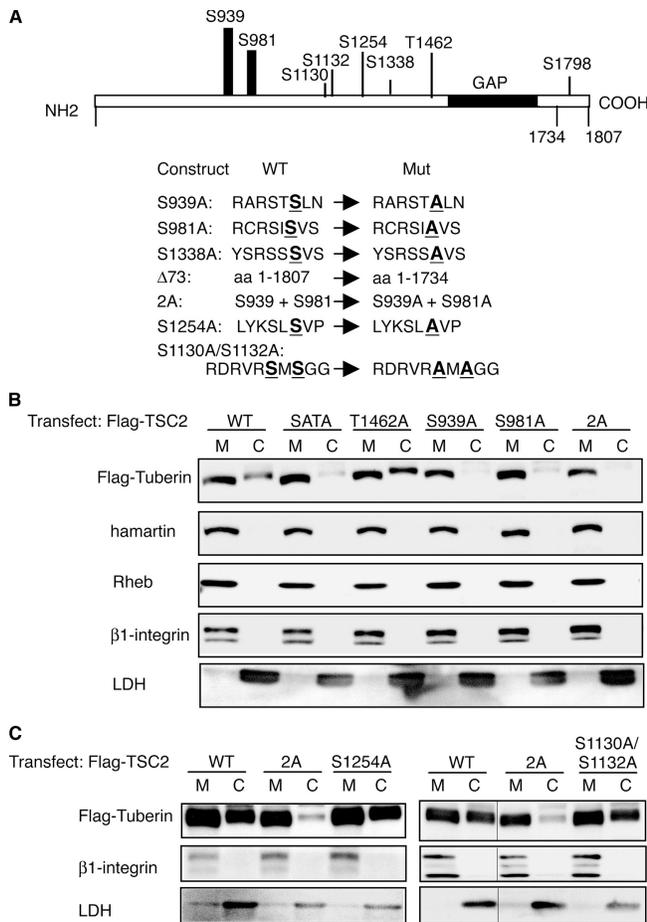
Flag-Tuberin

β1-integrin

LDH

Figure 3. **Identification of S939 and S981 as phosphorylation sites that determine tuberin localization.** (A) Schematic of tuberin phosphorylation sites with Flag-TSC2 constructs and their corresponding mutations listed below. (B) Western analysis of HEK293 membrane and cytosolic fractions using an anti-Flag antibody after transfection with wild-type and mutant Flag-TSC2 constructs. (C) Wild-type and mutant Flag-TSC2 constructs were overexpressed in HEK293 cells, and the membrane and cytosol lysates were immunoblotted with an anti-Flag antibody. The vertical line indicates nonadjacent lanes in a single blot.

Manning et al., 2002), S981 (Dan et al., 2002), S1130/S1132 (Inoki et al., 2002), and T1462 (Inoki et al., 2002; Manning et al., 2002) have been reported to be AKT phosphorylation sites in vivo and/or in vitro, and several of these also have the potential for binding to 14-3-3 (http://scansite.mit.edu; Yaffe et al., 2001). S981 is of particular interest, as it lies within the alternatively spliced exon 25 of tuberin. To examine these as candidate sites for the regulation of tuberin localization, we mutated these residues to alanine to create TSC2 constructs in frame with an NH$_2$-terminal Flag epitope (Flag-TSC2): S939A, S981A, and 2A (S939A + S981A); T1462A and SATA (S939A + T1462A; Manning et al., 2002); and S1254A and S1130A + S1132A double mutant.

Wild-type and mutant TSC2 constructs were transfected into HEK293 cells and subjected to subcellular fractionation. As shown in Fig. 3 (B and C), S939A, S981A, and 2A mutants predominantly localized to the membrane, as did the double alanine SATA mutant that lacks the S939 site. However, the T1462A single mutant partitioned in the cell similarly to wild-type tuberin (Fig. 3 B), indicating that T1462 phosphorylation

was not directing translocation of tuberin from the membrane to the cytosol. These data were confirmed with a phosphospecific T1462 antibody, which recognized tuberin in both the membrane and cytosolic fractions equally (unpublished data). Furthermore, phosphorylation at both S939 and S981 contributes to cytosolic localization, as phosphorylation at S939 (determined with a phospho-S939 specific antibody) of the S981A mutant was not sufficient to partition tuberin to the cytosol (Fig. S2 C). Other tuberin mutants, S1254A, S1130A/S1132A (Fig. 3 C), Δ73, or S1338A (Fig. S1 C), also distributed equally between the membrane and cytosolic fractions. Thus, S939 and S981 phosphorylation are critical determinants of membrane versus cytosolic localization of tuberin.

14-3-3 proteins mediate translocation of tuberin into the cytosol

14-3-3 has been previously reported to directly interact with phosphorylated tuberin (Li et al., 2002; Nellist et al., 2003). S939 and S981 are predicted AKT phosphorylation and 14-3-3 interaction sites. When phosphorylated and nonphosphorylated S939 and S981 peptides were used in competition assays to block GST–14-3-3 interaction with tuberin, as shown in Fig. 4 A and Fig. S3 (available at http://www.jcb.org/cgi/content/full/jcb.200507119/DC1), phosphorylated but not nonphosphorylated S939 and S981 peptides clearly competed for the interaction of tuberin with several 14-3-3 isoforms. In addition, the amount of 2A mutant tuberin affinity purified by 14-3-3 was dramatically reduced relative to wild-type tuberin (Fig. 4 B). Importantly, inhibition of PI3K signaling by wortmannin ablated this 14-3-3 tuberin interaction (Fig. 4 B). These data indicate that S939 and S981 are critical sites of interaction between tuberin and 14-3-3 proteins and that this interaction is mediated by PI3K/AKT phosphorylation.

To demonstrate that tuberin binding to 14-3-3 was directly responsible for its translocation to the cytosol, we transfected HEK293 cells with the EGFP-R18 construct that expresses a peptide that disrupts 14-3-3 binding (Jin et al., 2004). As shown in Fig. 4 C, the R18 14-3-3 decoy clearly repressed cytosolic localization of tuberin, establishing a direct link between 14-3-3 and translocation of tuberin to the cytosol.

Hamartin enhances tuberin retention at the membrane

Hamartin possesses a predicted transmembrane domain and two coiled-coil domains that mediate its association with tuberin (van Slegtenhorst et al., 1997, 1998). We found that in both human and mouse cells, hamartin was only detected in the membrane fraction (Fig. 5, A and B; Fig. 3 B; unpublished data). To confirm that tuberin mutants that did or did not constitutively localize to the membrane retained their ability to bind hamartin, immunoprecipitation experiments were performed. Immunoprecipitation showed that, similar to wild-type tuberin, tuberin S939A, S981A, S1338A, Δ73, and 2A mutants retained their ability to interact with hamartin (Fig. S4, A, B, and C, available at http://www.jcb.org/cgi/content/full/jcb.200507119/DC1). To determine whether hamartin played a role in the subcellular localization of tuberin, we transfected wild-type, S939A,
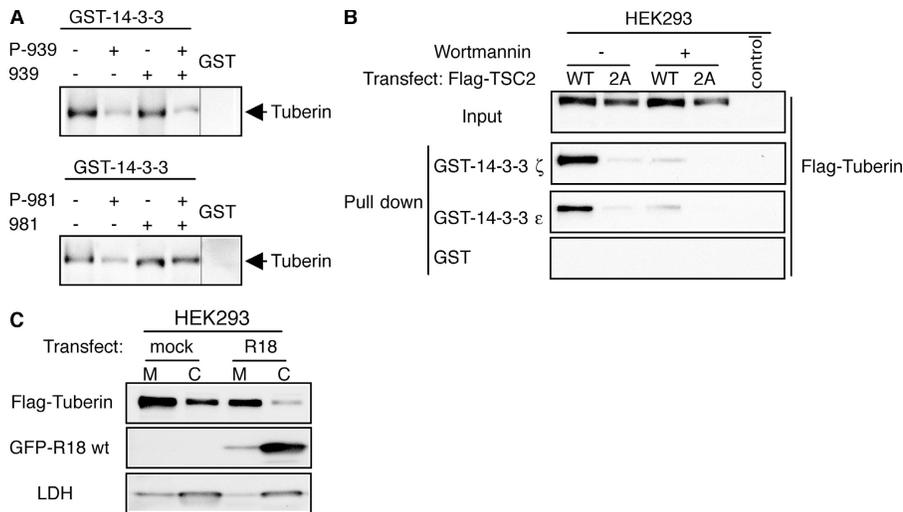
Figure 4. **14-3-3 proteins bind and sequester tuberin in the cytosol.** (A) GST–14-3-3 proteins were used to affinity purify proteins from HEK293 cells in the presence of phosphorylated or nonphosphorylated S939 and S981 tuberin peptides. Affinity-purified complexes were immunoblotted to detect the amount of tuberin interacting with 14-3-3. The vertical line indicates nonadjacent lanes in a single blot. (B) HEK293 cells were transfected with Flag-TSC2-WT or Flag-TSC2-2A in the absence or presence of 200 nM wortmannin. Western analysis of exogenous tuberin was performed after using GST–14-3-3 proteins to affinity purify Flag-tuberin. (C) HEK293 cells were transfected with Flag-TSC2 in the presence or absence of GFP-R18 14-3-3 decoy expression construct, and fractionated lysates were used for Western analyses with the indicated antibodies. LDH was used as a fractionation control.

and S981A Flag-TSC2 constructs into HEK293 cells with or without Myc- or Flag-TSC1. Although S939A and S981A mutants were primarily membrane localized, coexpression of hamartin increased membrane retention of both mutant and wild-type tuberin in a dose-dependent manner (Fig. 5, A and B). These data suggest that the interaction of hamartin with tuberin facilitates its localization to the membrane, implying that the tuberin–hamartin heterodimer functions in this subcellular compartment.

Importantly, only tuberin in the membrane fraction remained associated with hamartin: no hamartin could be co-immunoprecipitated with tuberin in the cytosolic fraction, indicating that translocation to the cytosol dissociated tuberin from hamartin (Fig. 5 C). Similarly, when Flag-TSC2 and Myc-TSC1 were cotransfected into MCF7 cells, tuberin and

hamartin were observed by confocal microscopy to colocalize in a discrete, punctate pattern (Fig. S4 D). Cells that expressed wild-type Flag-TSC2 in the absence of Myc-TSC1 exhibited a more diffuse staining pattern than cells that overexpressed both Myc-TSC1 and Flag-TSC2 (Fig. S4 D, comparing γ and γ′ with β and β′). However, the 2A mutant, which was constitutively membrane localized as shown by cell fractionation, retained this punctate localization pattern even in the absence of exogenously expressed hamartin (Fig. S4 E).

Colocalization of tuberin and Rheb is disrupted in response to growth factor stimulation

Tuberin's GAP target Rheb is farnesylated and predicted to be membrane localized (Clark et al., 1997), and recent data indicate
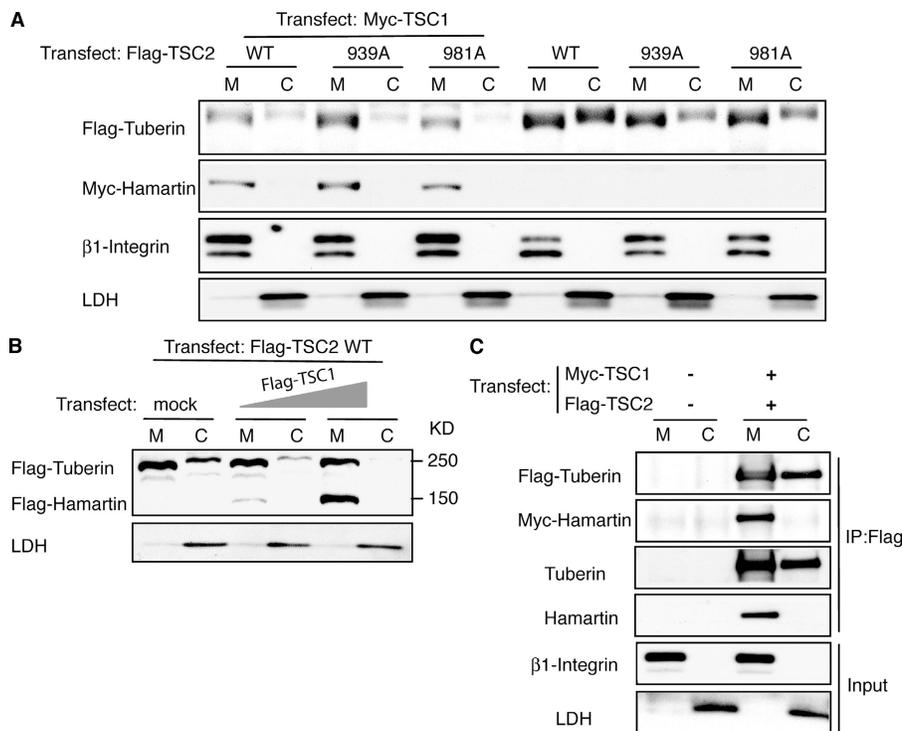

Figure 5. **Hamartin increases the amount of tuberin retained in the membrane.** (A) HEK293 cells were transfected with wild-type and mutant Flag-TSC2 constructs in the presence or absence of a Myc-TSC1 construct. Cells were fractionated and immunoblotted with indicated antibodies. (B) HEK293 cells were transfected with wild-type TSC2 constructs along with increasing amounts of Flag-TSC1. Cells were then fractionated and immunoblotted with indicated antibodies. (C) HEK293 cells were transfected with Flag-TSC2 and Myc-TSC1 constructs. The fractionated cell lysates were immunoprecipitated with an anti-Flag antibody followed by Western analysis with anti-Flag (mouse) and anti-Myc (mouse). The same blot was then reprobed with anti-tuberin (rabbit) and anti-hamartin (rabbit) as indicated.

Figure 6. **Tuberin colocalization with Rheb is disrupted in response to growth factor stimulation.** HeLa cells were transfected in serum-free media with Flag-TSC2 WT and Myc-Rheb along with an untagged TSC1 construct. After 12 h without serum, cells were treated with 30 ng/ml IGF-1 for 1 h. Localization of exogenous Flag-tuberin (green) and Myc-Rheb (red) was detected by double immunofluorescence labeling and confocal microscopy. Colocalization is detected in the merged image with the yellow signal (right).
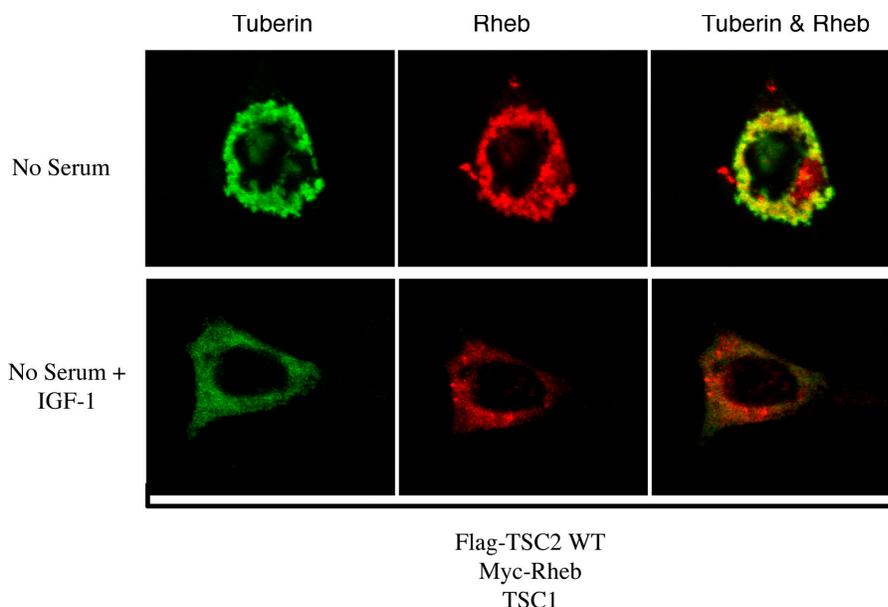
that Rheb is localized in endomembranes (Takahashi et al., 2005). To determine whether phosphorylation at S939/S981 affected tuberin's intrinsic GAP activity for Rheb, we first determined Rheb's subcellular localization. Rheb was detected only in the membrane fractions from HEK293 (Fig. 3 B) and MCF7 (Fig. S5 A, available at http://www.jcb.org/cgi/content/full/jcb.200507119/DC1) as well as NIH3T3, Swiss3T3, and TRKE2 cells (not depicted). Treatment with EGF or wortmannin did not affect this localization over a period of 10 min to 3 h (Fig. S5 A and not depicted). Recognition of the 21-kD band in the membrane fraction using this anti-Rheb antibody was specific for Rheb, as antibody binding was ablated when Rheb RNAi was used to knock down Rheb (Fig. S5 B). When untagged *TSC1*/Flag-*TSC2* and Myc-*Rheb* were cotransfected into HeLa cells, tuberin and Rheb were observed with confocal microscopy to colocalize in a discrete, punctate pattern in the absence of serum (Fig. 6). In contrast, stimulation with IGF-1 resulted in partitioning of wild-type tuberin away from Rheb (Fig. 6), indicating that in response to growth factor stimulation, tuberin is no longer retained in physical proximity to its downstream target, Rheb. Collectively, these data indicate that the localization pattern of tuberin is modulated by both hamartin and growth factor signaling and that Rheb is in physical proximity to membrane-localized tuberin and hamartin within the cell. In addition, these data, along with confocal microscopy using 2A mutant tuberin and biochemical fractionation, suggest that S939 and S981 are crucial sites for determining the subcellular localization and, thus, function of tuberin in response to growth factor signaling.

Tuberin localization regulates its function

To elucidate the relationship between tuberin localization and function, we examined the effect of wild-type, S939A, S981A, and 2A tuberin mutants on mTOR-S6K activity. T389 is a known rapamycin-sensitive phosphorylation site of S6K that correlates with activation by mTOR (Pearson et al., 1995).

In cells transfected with HA-tagged S6K, cotransfection of wild-type *TSC1* and *-2* expression constructs diminished phosphorylation of exogenously expressed S6K (Fig. 7 A). However, cotransfection of the 2A mutant with *TSC1* resulted in an even more dramatic reduction in phospho-S6K levels (Fig. 7 A). Similar experiments were performed to determine the effect of S939A and S981A single and double mutants on phosphorylation of endogenous S6K. In the presence of serum, wild-type Flag-tuberin was located in the membrane and cytosol, whereas S939A, S981A, and 2A Flag-tuberin mutants remained primarily at the membrane (Fig. 7 B, top). AKT was equally activated by serum in cells expressing wild-type or mutant tuberin constructs, and endogenous hamartin remained membrane localized (Fig. 7 B). In cells transfected with wild-type tuberin, phosphorylation of endogenous S6K at T389 increased in response to serum, coincident with translocation of tuberin to the cytosol. However, in cells transfected with S939A, S981A, or 2A tuberin mutants, phosphorylation of S6K was inhibited, with the 2A mutant most effectively blocking S6K activation (Fig. 7 B). Thus, tuberin mutants that were retained at the membrane were constitutively active and exhibited enhanced ability to repress S6K activation. These data suggest that AKT phosphorylation of tuberin regulates its activity by decreasing the amount of tuberin located at the membrane, thereby reducing its inhibitory effect on the Rheb–mTOR–S6K signaling pathway.

Phosphorylation sites that determine localization and function of tuberin do not change its intrinsic RhebGAP activity in vitro

Physical sequestration of tuberin from its target Rheb suggested a mechanism whereby AKT modulated tuberin by partitioning it away from the membrane rather than altering its intrinsic GAP activity for Rheb. We compared the relative RhebGAP activity of wild-type TSC2 and 2A mutant (S939A and S981A) in cells during activation of the PI3K–AKT pathway (Fig. 8).
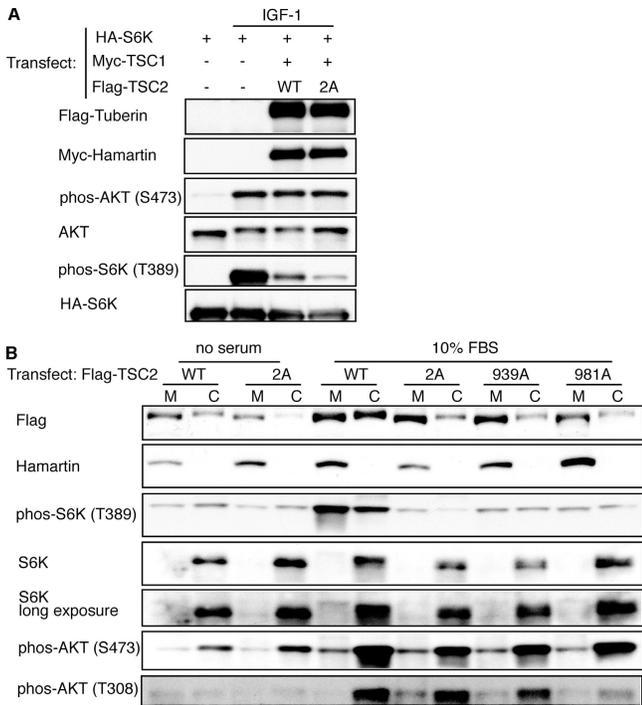
Figure 7. **AKT-mediated phosphorylation of tuberin relieves repression of mTOR-S6K signaling.** (A) HEK293 cells were transfected with HA-S6K, Myc-TSC1, and Flag-TSC2 constructs as indicated. Cells were serum starved for 24 h and treated with or without 30 ng/ml IGF-1 for 1 h. Cell lysates were immunoblotted with the indicated antibodies, and phopho-S6K levels were compared with the amount of HA-S6K protein levels. Phospho-AKT (S473) was blotted as a control for the effectiveness of IGF-1 treatment. (B) Western analyses of membrane and cytosolic fractions from HEK293 cells transfected with wild-type or mutant Flag-TSC2 constructs. After 9 h, serum was either removed or allowed to remain for 24 h. The protein levels of phosphorylated endogenous S6K were compared with total S6K protein levels. Phospho-AKT (S473) and phospho-AKT (T308) were blotted as controls for the effectiveness of the indicated treatments.

To do this, we quantified the ratio of GTP and GDP Myc-Rheb (percentage of GTP bound Myc-Rheb) when these TSC2 constructs were coexpressed during a time course of insulin stimulation. The 2A mutant enhanced the GTPase function of Rheb more effectively than wild-type tuberin, as indicated by impaired accumulation of the active GTP form of Rheb after 15 min of insulin stimulation (32% GTP bound) when compared with wild-type TSC2 (42% GTP bound; Fig. 8 A). As an increase in GTP bound Rheb would be predicted to enhance mTOR-mediated cell signaling, we measured the activity of HA-S6K1 in these cells (Fig. 8 B). As expected, insulin-induced activation of S6K1 was markedly impaired in cells expressing the 2A mutant with the 2A mutant blocking insulin-induced activation of S6K1 by 50% (after 15 min) when compared with wild-type TSC2 (Fig. 8 B), reflecting the reduced levels of active GTP bound Rheb (Fig. 8 A).

To determine whether phosphorylation at S939 and S981 had an impact on tuberin's intrinsic GAP activity, we analyzed the ability of wild-type or mutant tuberin proteins to activate Rheb GTPase in vitro. RhebGAP assays were conducted on immunoprecipitated tuberin–hamartin heterodimers containing either the wild-type or AKT-phosphorylation mutants of TSC2 (Fig. 9).
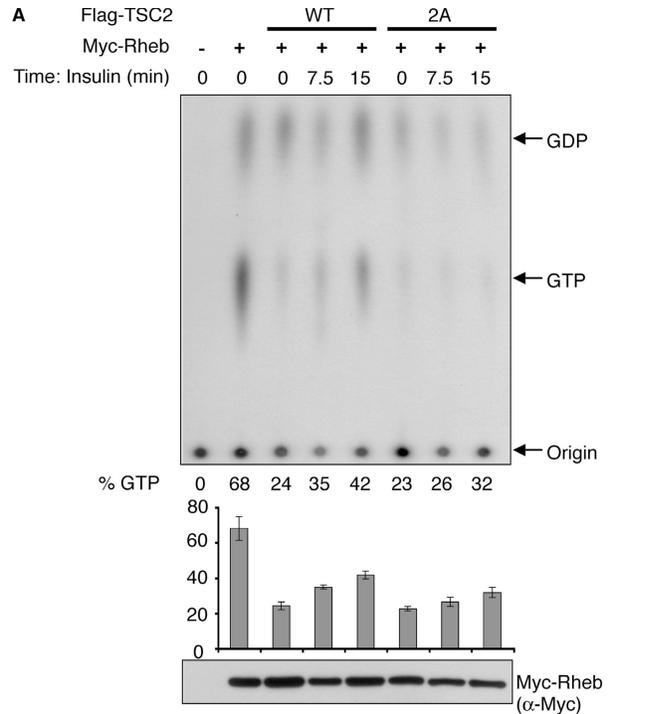

Figure 8. **AKT phosphorylation of tuberin promotes Rheb-induced S6K1 activation through increased Rheb-GTP loading.** (A) HEK293 cells co-expressing HA-S6K1, Myc-Rheb, Flag-TSC1, and either Flag-TSC2-WT or Flag-TSC2-2A (S939A and S981A) were serum starved and, where indicated, the PI3K–AKT signaling pathway was stimulated with 100 nM insulin for 7.5 and 15 min. These cells were subjected to in vivo radiolabeling, and the level of guanine nucleotide bound to immunoprecipitated Myc-Rheb was quantified. A representative blot from three independent biological replications is shown. The mean of the percentage of total Myc-Rheb bound to GTP (active state) is shown in the bar figure. (B) In parallel, HEK293 cells treated as in A were subjected to S6K1 activity assays. HA-S6K1 used in the activity assay was analyzed with an anti-HA antibody. ^{32}P-incorporation into GST-S6 substrate was quantified using a phospho-rimager, and the fold activation of S6K1 is graphed. Protein levels of Flag-TSC1, Flag-TSC2, and AKT, and level of AKT phosphorylation at S473, were determined using Western analyses.
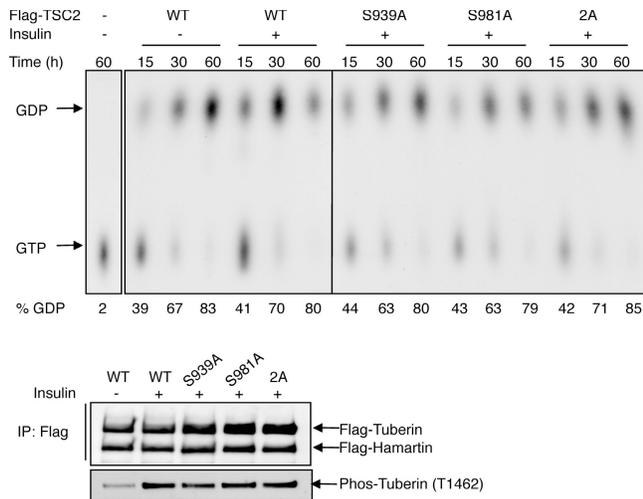
Figure 9. **Tuberin's GAP activity for Rheb in vitro is not affected by AKT phosphorylation.** HEK293 cells coexpressing Flag-TSC1 and Flag-TSC2-WT, Flag-TSC2-S939A, Flag-TSC2-S981A, or Flag-TSC2-2A were serum starved and then stimulated with 100 nM insulin for 30 min. TSC1 and -2 were immunoprecipitated from the lysates and subjected to RhebGAP activity assays for 15, 30, or 60 min. Immunocomplexes containing wild-type and mutant tuberin activated Rheb similarly, as indicated by quantitation of percentage of GDP. The vertical line indicates nonadjacent lanes resolved on a single thin layer chromatography plate. For quality control of the α-[^{32}P]GTP used in the assay, the guanine nucleotide eluted from the 60-min vector control was resolved on a separate thin layer chromatography plate and shows that Rheb is 98% bound to GTP in the absence of hamartin and tuberin. Each assay contained approximately equal amounts of TSC1 and -2, and AKT activation was confirmed with a phospho-T1462 antibody by Western blot analysis (bottom).

Figure 10. **Model for regulation of tuberin under conditions of mitogenic sufficiency.** (A) Tuberin normally functions as a GAP for Rheb within an intracellular membrane compartment, inhibiting Rheb and mTOR signaling, which suppresses cell growth. (B) Upon stimulation by growth factors, AKT is activated, leading to phosphorylation and cytosolic sequestration of tuberin by 14-3-3 proteins. This cytosolic translocation relieves tuberin repression of the Rheb-mTOR signaling, stimulating cell growth.

Tuberin–hamartin complexes containing wild-type tuberin from both unstimulated and insulin-stimulated cells enhanced the intrinsic GTPase activity of Rheb at comparable rates. Induction of tuberin phosphorylation by insulin was confirmed in these lysates by detection of phospho-T1462 (Fig. 9, bottom). Furthermore, tuberin mutants lacking these sites (S939A, S981A, and 2A) also possessed similar RhebGAP activity to wild-type tuberin in vitro, even after insulin treatment (Fig. 9). These findings imply that AKT-mediated phosphorylation of tuberin does not directly alter the rates at which tuberin enhances the GTPase activity of Rheb, at least in vitro. However, these data support a mechanism whereby AKT phosphorylation suppresses tuberin function by translocating tuberin to the cytosol away from its membrane-associated binding partner, hamartin, and its downstream target, Rheb. Indeed, as the efficiency with which tuberin functions as a RhebGAP in vitro is significantly reduced in the absence of hamartin, physical separation from both hamartin and Rheb may be contributing to reduced tuberin activity (Tee et al., 2002; Li et al., 2004b).

A mechanism by which tuberin function is regulated through subcellular localization

Based on our data, we propose a model where in the absence of growth stimulatory signals, hamartin facilitates localization of hypophosphorylated tuberin to membranes in physical proximity to Rheb. The membrane-associated tuberin–hamartin complex binds Rheb and acts as a GAP to inactivate membrane
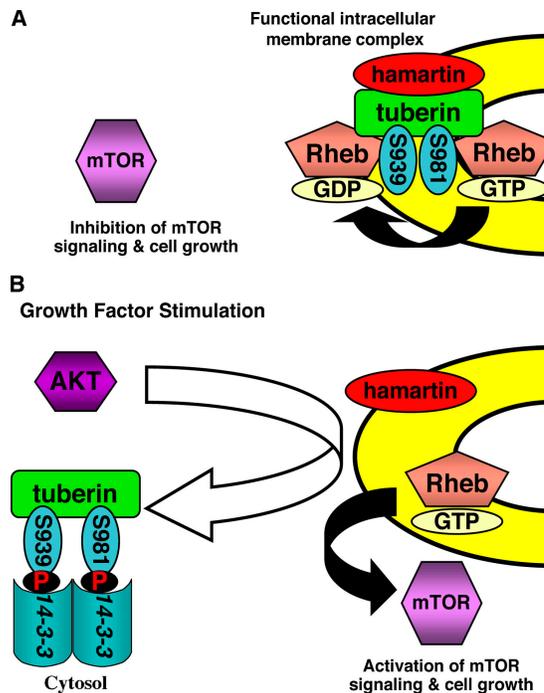
Rheb signaling by stimulating GTP hydrolysis (Fig. 10 A). However, during mitogenic sufficiency (i.e., after growth factor stimulation), activation of PI3K signaling leads to activation of AKT, which then directly phosphorylates membrane-associated tuberin. In response to AKT phosphorylation, 14-3-3 proteins bind tuberin and sequester it in the cytosol. The deficiency of membrane-associated tuberin results in the accumulation of GTP bound Rheb, which leads to increased mTOR signaling, enhanced cell growth, and proliferation (Fig. 10 B).

Discussion

In this study, we provide evidence that AKT inhibits the tumor suppressor function of tuberin by altering its subcellular localization. Previously, AKT was shown to directly phosphorylate and inhibit tuberin function upon stimulation with growth factors (Marygold and Leevers, 2002). However, it was not known how AKT phosphorylation of tuberin regulated its function or how hamartin contributed to tuberin regulation of Rheb and mTOR (Garami et al., 2003; Tee et al., 2003; Zhang et al., 2003). We have shown that although tuberin is found in both the membrane and cytosolic fractions of cells, cytosolic tuberin accumulates upon growth factor stimulation and is hyperphosphorylated. The translocation of tuberin from the membrane to the cytosol can be blocked by PI3K inhibitors, and AKT-phosphorylated tuberin is predominantly found in cytosolic fractions. The AKT phosphorylation sites S939 and S981 are

crucial residues that affect tuberin localization, with localization of tuberin to the membrane accounting for the ability of tuberin to inhibit mTOR signaling via its GAP activity for Rheb.

We show that two tuberin phosphorylation sites, S939 and S981, are responsible for interaction with 14-3-3 in a phosphorylation-dependent manner. 14-3-3 proteins are highly acidic dimeric intracellular proteins that chiefly bind to phosphoserine motifs (Yaffe and Elia, 2001). They play a key regulatory role in many cellular processes, including signal transduction, apoptosis, and cell cycle checkpoint control (Muslin and Xing, 2000; Tzivion et al., 2001; Yaffe, 2002; Hermeking, 2003). In many instances, 14-3-3 binding leads to altered subcellular localization of target proteins, which modulates their function. As this appears to be the case for tuberin as well, we propose a mechanism whereby growth factor stimulation activates AKT, leading to tuberin phosphorylation and mislocalization within the cell. Although some studies have suggested that the tuberin–hamartin heterodimer is destabilized upon AKT-mediated phosphorylation of tuberin (Inoki et al., 2002; Potter et al., 2002), our data and those of others indicate that AKT-mediated phosphorylation of tuberin does not change its affinity for hamartin (Dan et al., 2002; Manning et al., 2002; Tee et al., 2003). An alternative hypothesis is that in response to phosphorylation of S939 and S981 by AKT, 14-3-3 binds to these phosphorylated motifs to localize tuberin in the cytosol, physically sequestering tuberin away from hamartin. The presence of two adjacent 14-3-3 binding sites at S939 and S981 of tuberin may be important, as they would be predicted to stabilize binding of tuberin in the central channel of the 14-3-3 dimer more effectively than would a single binding site.

In this regard, it is interesting that loss of either the S939 or S981 14-3-3 binding sites reduces localization of tuberin to the cytosol. As one of these binding sites is in the alternatively spliced exon 25 of tuberin, it suggests that alternative splicing may allow for wider or more varied regulation of this tumor suppressor. In splice isoforms lacking exon 25, the absence of the S981 binding site could result in retention at the membrane, potentially enhancing tuberin activity. This could provide a mechanism via alternative exon splicing for cells and tissues to regulate tuberin localization and function. It might be noted that in previous studies that failed to identify the S939 site within tuberin as a 14-3-3 binding site, the TSC2 construct used lacked the alternatively spliced exon 25 and the S981 14-3-3 binding site (Li et al., 2002).

Hamartin has been shown to significantly enhance tuberin's GAP activity toward Rheb GTPase (Garami et al., 2003; Tee et al., 2003), and our observations also emphasize the importance of the interaction between tuberin and hamartin as a functional unit. We found that hamartin directly interacts with tuberin and promotes tuberin colocalization at the membrane in proximity to its GAP target Rheb and enhances tuberin's ability to repress mTOR signaling. Both endogenously and exogenously expressed hamartin were detected in the membrane fraction of cells, even when cells were treated with serum or growth factors, data that are consistent with the previous reports that hamartin is a membrane protein (van Slegtenhorst et al., 1997; Plank et al., 1998). The colocalization of tuberin in proximity to

its activation partner hamartin and its GAP target Rheb at the membrane could explain why increased retention of tuberin at the membrane enhances its ability to inhibit phosphorylation of S6K. Given that the S939 and S981 residues lie distal from the COOH-terminal GAP region (residues 1517–1674) of tuberin and mutation of these sites does not affect the Rheb GAP activity of tuberin, we conclude that phosphorylation of S939 and S981 does not directly regulate the GAP function of TSC2. However, mutation of these sites significantly inhibits Rheb-induced S6K1 activation through decreased Rheb-GTP loading, suggesting that AKT regulates tuberin function by causing tuberin translocation to the cytosol, rather than by directly inhibiting its intrinsic GAP activity toward Rheb.

Materials and methods

Antibodies and reagents
The following antibodies were used: tuberin, hamartin, lamin A/C, HA, and Myc (Santa Cruz Biotechnology, Inc.); Rheb, phosphotuberin (T1462), S6K, phospho-S6K (T389), AKT, phospho-AKT (S473), phospho-AKT (T308), and phospho-(S/T) AKT substrate (Cell Signaling Technology); Flag M2 and Flag M2 immobilized agarose beads (Sigma-Aldrich); LDH (Chemicon International); EGFP (Abcam); and β1-integrin (CLONTECH Laboratories, Inc.). The following reagents were used: EGF, insulin, and wortmannin (Sigma-Aldrich) and IGF-1 (R & D Systems). Tuberin peptides were synthesized by W.M. Keck Biotechnology Resource Center.

Constructs
Full-length human TSC1 and -2 cDNAs (supplied by J. DeClue, National Cancer Institute, Bethesda, MD) were subcloned into pcDNA3.1 (Invitrogen) and pCMV-Tag2 (Stratagene) expression vectors with NH$_2$-terminal Myc or Flag epitopes, respectively. COOH-terminal truncation mutant of TSC2 (Δ73) (residues 1–1734) was created by EcoR V digestion followed by religation. TSC2 mutations were generated by site-directed mutagenesis (Stratagene).

Other constructs used in this study were generously provided as follows: Flag-TSC1 and HA-S6K from J. Blenis (Harvard Medical School, Boston, MA), HA-RSK1 from J. Avruch (Massachusetts General Hospital, Boston, MA), GFP-R18 from T. Pawson (Mount Sinai Hospital, Toronto, Canada), and the Flag-TSC2 SATA and T1462A from B. Manning (Harvard School of Public Health, Boston, MA). GST–14-3-3 constructs were described previously (Liu et al., 2002).

Cell culture, transfection, and immunoprecipitation
Cell lines were grown as follows: MCF7 cells were grown in improved minimum essential medium (Biosource International). TRKE2 cells were grown in DF8 complete medium (Walker and Ginsler, 1992). HeLa cells were grown in MEM, and HEK293, Swiss3T3, and NIH3T3 cells were grown in DME (Life Technologies, Inc.). All media contained 10% FBS (Hyclone) unless otherwise noted. Myr-Akt MCF7 cells were cultured as previously described (DeGraffenried et al., 2003). Transfections were performed using the Lipofectamine 2000 reagent (Invitrogen) according to manufacturer's instructions. Cells were lysed using PBS containing 0.1% SDS, 1% NP-40, 0.5% deoxycholic acid, 1 μM PMSF, 20 μg/ml aprotinin, 10 μM leupeptin, and 1 μM Na$_3$VO$_4$. For immunoprecipitation, cell lysates were immunoprecipitated with the indicated antibodies and protein A– or protein G–Sepharose beads (GE Healthcare) and washed with buffer (10 mM Tris-HCl, pH 7.5, 1% NP-40, 1% Triton X-100, 100 mM NaCl, 50 mM NaF, 2 mM EDTA, 1 mM PMSF, and Complete protease inhibitor cocktail [Roche]). Immunocomplexes were subjected to SDS-PAGE and Western blotting.

Subcellular fractionation and protein phosphatase treatments
Cells (70–80% confluent in 15-cm plates) were washed and collected by scraping into ice-cold PBS, pelleted by centrifugation at 4°C, resuspended in hypotonic buffer (10 mM Hepes, pH 7.2, 10 mM KCl, 1.5 mM MgCl$_2$, 0.1 mM EGTA, 20 mM NaF, and 100 μM Na$_3$VO$_4$), and disrupted using a Dounce homogenizer. Crude nuclei and unbroken cells were then pelleted by centrifugation at 3,000 rpm at 4°C for 5 min. The postnuclear supernatant was separated by ultracentrifugation at 100,000 g for 1 h at 4°C. The supernatant, or cytosolic fraction, was removed and the pellet

was lysed in 1× lysis buffer (20 mM Tris-HCl, pH 7.5, 150 mM NaCl, 1 mM EDTA, 1 mM EGTA, 1% Triton X-100, 2.5 mM $NA_4P_2O_7$, 1 mM β-glycerophosphate, 1 mM Na_3VO_4, and 1 µg/ml leupetin). The insoluble fractions were removed by centrifugation at 14,000 rpm for 10 min, and the supernatant was collected as the membrane fraction. Crude nuclei were resuspended with hypotonic buffer and homogenized using a Dounce homogenizer. After centrifugation at 4°C for 5 min, the pellet was further washed with wash buffer (10 mM Tris-HCl, pH 7.4, 0.1% NP-40, 0.05% sodium deoxycholate, 10 mM NaCl, and 3 mM $MgCl_2$) and lysed in high-salt lysis buffer (20 mM Hepes, pH 7.4, 0.5 M NaCl, 0.5% NP-40, and 1.5 mM $MgCl_2$). All lysis and wash buffers contained 1× Complete protease inhibitor cocktail. The nuclear, membrane, and cytosolic lysates were normalized using the BCA Protein Assay kit (Pierce Chemical Co.) and subjected to SDS-PAGE and immunoblot analysis. For phosphatase treatment, equal amounts of membrane and cytosolic lysates were treated with CIAP serine/threonine phosphatase or YOP tyrosine phosphatase at 30°C for 1 h.

GST–14-3-3 pull-down assays
GST pull-down assays were performed as previously described (Liu et al., 2002). For peptide competition assays, incubations were performed in the presence or absence of 100 µM phospho-Ser[939] or Ser[939] tuberin peptide (SGSGFRARSTS [939] LNERPK) or phospho-Ser[981] or Ser[981] tuberin peptide (SGSGFRCRSIS [981] VSEHVV).

Rheb GAP and S6K1 assay
Anti-Flag M2 antibody was used to immunoprecipitate Flag-tuberin from HEK293E cells. Immunocomplexes of TSC1/TSC2 were used for in vitro RhebGAP assays as previously described (Tee et al., 2003). α-[^{32}P]GTP and α-[^{32}P]GDP were eluted from Rheb and resolved by thin layer chromatography on PEI cellulose (Sigma-Aldrich) with KH_2PO_4. The relative levels of radiolabeled GTP and GDP were quantified with a phosphorimager.

S6K1 activity assays on immunoprecipitated HA-S6K1 were performed as previously described (Martin et al., 2001) using recombinant GST-S6 (32 COOH-terminal amino acids of ribosomal protein S6) as substrate.

In vivo Rheb nucleotide binding
Analysis of Rheb guanine nucleotide binding in cells was determined as previously described (Tee et al., 2005).

Immunofluorescent staining
Intracellular localization of wild-type tuberin and 2A mutant and colocalization studies was determined by immunofluorescence analysis of HeLa cells. Transfected cells were plated onto glass chamber slides in the absence of serum. After 12 h of serum starvation, transfected cells were treated with either 20% FBS or 30 ng/ml IGF-1 for 1 h. Cells were then fixed in 50% ethanol plus 10% acetic acid for 1 h at 4°C, and nonspecific antigens were blocked for 1 h in PBS containing 7.5% BSA at 37°C. Rabbit anti-Flag (Sigma-Aldrich) and/or mouse anti-Myc (Santa Cruz Biotechnology, Inc.) primary antibodies were incubated in PBS/7.5% BSA at 37°C for 2 h. Primary antibodies were detected with FITC-conjugated goat anti–rabbit (Abcam) and Cy3-conjugated donkey anti–mouse (Jackson ImmunoResearch Laboratories) antibodies, respectively.

Microscopy
Fluorescence images were analyzed either on a confocal microscope (Fluoview Scanning Laser Biological Microscope IX 70 system; Olympus) equipped with two lasers (Ar 488 and Kr-Ar 488–564) using UplanFl 100× oil-immersion (NA 1.30) objective or a conventional microscope with fluorescence attachment (BX40 attached with BX-FLA; Olympus) using UplanFl 40× (NA 0.75) objective. Fluoview version 1.26 software (Olympus) and MagnaFire version 2.1C (Olympus) were used for image acquisition from confocal microscopy and conventional microscopy, respectively. Photoshop 8.0 software (Adobe) was used for minor adjustments and processing of images.

Online supplemental material
Fig. S1 shows that AKT-mediated phosphorylation of tuberin leads to subcellular translocation. Fig. S2 shows that S939 and S981 are required for altered subcellular localization of tuberin. Fig. S3 demonstrates that 14-3-3 proteins bind phosphorylated S939 and S981 residues. Fig. S4 demonstrates that tuberin mutants retain their ability to interact with hamartin. Fig. S5 shows that Rheb is retained in the membrane fraction in the presence or absence of growth factor treatment. Online supplemental material is available at http://www.jcb.org/cgi/content/full/jcb.200507119/DC1.

References

Alessi, D.R., F.B. Caudwell, M. Andjelkovic, B.A. Hemmings, and P. Cohen. 1996. Molecular basis for the substrate specificity of protein kinase B; comparison with MAPKAP kinase-1 and p70 S6 kinase. *FEBS Lett.* 399:333–338.

Ballif, B.A., P.P. Roux, S.A. Gerber, J.P. MacKeigan, J. Blenis, and S.P. Gygi. 2005. Quantitative phosphorylation profiling of the ERK/p90 ribosomal S6 kinase-signaling cassette and its targets, the tuberous sclerosis tumor suppressors. *Proc. Natl. Acad. Sci. USA.* 102:667–672.

Bjornsti, M.A., and P.J. Houghton. 2004. The TOR pathway: a target for cancer therapy. *Nat. Rev. Cancer.* 4:335–348.

Cheadle, J.P., M.P. Reeve, J.R. Sampson, and D.J. Kwiatkowski. 2000. Molecular genetic advances in tuberous sclerosis. *Hum. Genet.* 107:97–114.

Clark, G.J., M.S. Kinch, K. Rogers-Graham, S.M. Sebti, A.D. Hamilton, and C.J. Der. 1997. The Ras-related protein Rheb is farnesylated and antagonizes Ras signaling and transformation. *J. Biol. Chem.* 272:10608–10615.

Dan, H.C., M. Sun, L. Yang, R.I. Feldman, X.M. Sui, C.C. Ou, M. Nellist, R.S. Yeung, D.J. Halley, S.V. Nicosia, et al. 2002. Phosphatidylinositol 3-kinase/Akt pathway regulates tuberous sclerosis tumor suppressor complex by phosphorylation of tuberin. *J. Biol. Chem.* 277:35364–35370.

DeGraffenried, L.A., W.E. Friedrichs, L. Fulcher, G. Fernandes, J.M. Silva, J.M. Peralba, and M. Hidalgo. 2003. Eicosapentaenoic acid restores tamoxifen sensitivity in breast cancer cells with high Akt activity. *Ann. Oncol.* 14:1051–1056.

The European Chromosome 16 Tuberous Sclerosis Consortium. 1993. Identification and characterization of the tuberous sclerosis gene on chromosome 16. *Cell.* 75:1305–1315.

Garami, A., F.J. Zwartkruis, T. Nobukuni, M. Joaquin, M. Roccio, H. Stocker, S.C. Kozma, E. Hafen, J.L. Bos, and G. Thomas. 2003. Insulin activation of Rheb, a mediator of mTOR/S6K/4E-BP signaling, is inhibited by TSC1 and 2. *Mol. Cell.* 11:1457–1466.

Gomez, M.R., J.R. Sampson, and V.H. Whittemore. 1999. Tuberous sclerosis complex. *In* Developmental Perspectives in Psychiatry. J.C. Harris, editor. Oxford University Press, Oxford, UK. 10–23, 275–312.

Hengstschlager, M., D.M. Rodman, A. Miloloza, E. Hengstschlager-Ottnad, M. Rosner, and M. Kubista. 2001. Tuberous sclerosis gene products in proliferation control. *Mutat. Res.* 488:233–239.

Hermeking, H. 2003. The 14-3-3 cancer connection. *Nat. Rev. Cancer.* 3:931–943.

Hodges, A.K., S. Li, J. Maynard, L. Parry, R. Braverman, J.P. Cheadle, J.E. DeClue, and J.R. Sampson. 2001. Pathological mutations in TSC1 and TSC2 disrupt the interaction between hamartin and tuberin. *Hum. Mol. Genet.* 10:2899–2905.

Inoki, K., Y. Li, T. Zhu, J. Wu, and K.L. Guan. 2002. TSC2 is phosphorylated and inhibited by Akt and suppresses mTOR signalling. *Nat. Cell Biol.* 4:648–657.

Inoki, K., M.N. Corradetti, and K.L. Guan. 2005. Dysregulation of the TSC-mTOR pathway in human disease. *Nat. Genet.* 37:19–24.

Jin, J., F.D. Smith, C. Stark, C.D. Wells, J.P. Fawcett, S. Kulkarni, P. Metalnikov, P. O'Donnell, P. Taylor, L. Taylor, et al. 2004. Proteomic, functional, and domain-based analysis of in vivo 14-3-3 binding proteins involved in cytoskeletal regulation and cellular organization. *Curr. Biol.* 14:1436–1450.

Li, Y., K. Inoki, R. Yeung, and K.L. Guan. 2002. Regulation of TSC2 by 14-3-3 binding. *J. Biol. Chem.* 277:44593–44596.

Li, Y., K. Inoki, P. Vacratsis, and K.L. Guan. 2003. The p38 and MK2 kinase cascade phosphorylates tuberin, the tuberous sclerosis 2 gene product, and enhances its interaction with 14-3-3. *J. Biol. Chem.* 278:13663–13671.

Li, Y., M.N. Corradetti, K. Inoki, and K.L. Guan. 2004a. TSC2: filling the GAP in the mTOR signaling pathway. *Trends Biochem. Sci.* 29:32–38.

Li, Y., K. Inoki, and K.L. Guan. 2004b. Biochemical and functional characterizations of small GTPase Rheb and TSC2 GAP activity. *Mol. Cell. Biol.* 24:7965–7975.

Liu, M.Y., S. Cai, A. Espejo, M.T. Bedford, and C.L. Walker. 2002. 14-3-3 interacts with the tumor suppressor tuberin at Akt phosphorylation site(s). *Cancer Res.* 62:6475–6480.

Lou, D., N. Griffith, and D.J. Noonan. 2001. The tuberous sclerosis 2 gene product can localize to nuclei in a phosphorylation-dependent manner. *Mol. Cell Biol. Res. Commun.* 4:374–380.

Manning, B.D., and L.C. Cantley. 2003. United at last: the tuberous sclerosis complex gene products connect the phosphoinositide 3-kinase/Akt pathway to mammalian target of rapamycin (mTOR) signalling. *Biochem. Soc. Trans.* 31:573–578.

Manning, B.D., A.R. Tee, M.N. Logsdon, J. Blenis, and L.C. Cantley. 2002. Identification of the tuberous sclerosis complex-2 tumor suppressor gene product tuberin as a target of the phosphoinositide 3-kinase/akt pathway. *Mol. Cell.* 10:151–162.

Martin, K.A., S.S. Schalm, C. Richardson, A. Romanelli, K.L. Keon, and J. Blenis. 2001. Regulation of ribosomal S6 kinase 2 by effectors of the phosphoinositide 3-kinase pathway. *J. Biol. Chem.* 276:7884–7891.

Marygold, S.J., and S.J. Leevers. 2002. Growth signaling: TSC takes its place. *Curr. Biol.* 12:R785–R787.

Muslin, A.J., and H. Xing. 2000. 14-3-3 proteins: regulation of subcellular localization by molecular interference. *Cell. Signal.* 12:703–709.

Nellist, M., M.A. van Slegtenhorst, M. Goedbloed, A.M. van den Ouweland, D.J. Halley, and P. van der Sluijs. 1999. Characterization of the cytosolic tuberin-hamartin complex. Tuberin is a cytosolic chaperone for hamartin. *J. Biol. Chem.* 274:35647–35652.

Nellist, M., M.A. Goedbloed, and D.J. Halley. 2003. Regulation of tuberous sclerosis complex (TSC) function by 14-3-3 proteins. *Biochem. Soc. Trans.* 31:587–591.

Obata, T., M.B. Yaffe, G.G. Leparc, E.T. Piro, H. Maegawa, A. Kashiwagi, R. Kikkawa, and L.C. Cantley. 2000. Peptide and protein library screening defines optimal substrate motifs for AKT/PKB. *J. Biol. Chem.* 275:36108–36115.

Pearson, R.B., P.B. Dennis, J.W. Han, N.A. Williamson, S.C. Kozma, R.E. Wettenhall, and G. Thomas. 1995. The principal target of rapamycin-induced p70s6k inactivation is a novel phosphorylation site within a conserved hydrophobic domain. *EMBO J.* 14:5279–5287.

Plank, T.L., R.S. Yeung, and E.P. Henske. 1998. Hamartin, the product of the tuberous sclerosis 1 (TSC1) gene, interacts with tuberin and appears to be localized to cytoplasmic vesicles. *Cancer Res.* 58:4766–4770.

Potter, C.J., L.G. Pedraza, and T. Xu. 2002. Akt regulates growth by directly phosphorylating Tsc2. *Nat. Cell Biol.* 4:658–665.

Roux, P.P., B.A. Ballif, R. Anjum, S.P. Gygi, and J. Blenis. 2004. Tumor-promoting phorbol esters and activated Ras inactivate the tuberous sclerosis tumor suppressor complex via p90 ribosomal S6 kinase. *Proc. Natl. Acad. Sci. USA.* 101:13489–13494.

Takahashi, K., M. Nakagawa, S.G. Young, and S. Yamanaka. 2005. Differential membrane localization of ERas and Rheb, two Ras-related proteins involved in the phosphatidylinositol 3-kinase/mTOR pathway. *J. Biol. Chem.* 280:32768–32774.

Tee, A.R., D.C. Fingar, B.D. Manning, D.J. Kwiatkowski, L.C. Cantley, and J. Blenis. 2002. Tuberous sclerosis complex-1 and -2 gene products function together to inhibit mammalian target of rapamycin (mTOR)-mediated downstream signaling. *Proc. Natl. Acad. Sci. USA.* 99:13571–13576.

Tee, A.R., B.D. Manning, P.P. Roux, L.C. Cantley, and J. Blenis. 2003. Tuberous sclerosis complex gene products, Tuberin and Hamartin, control mTOR signaling by acting as a GTPase-activating protein complex toward Rheb. *Curr. Biol.* 13:1259–1268.

Tee, A.R., J. Blenis, and C.G. Proud. 2005. Analysis of mTOR signaling by the small G-proteins, Rheb and RhebL1. *FEBS Lett.* 579:4763–4768.

Tzivion, G., Y.H. Shen, and J. Zhu. 2001. 14-3-3 proteins; bringing new definitions to scaffolding. *Oncogene.* 20:6331–6338.

van Slegtenhorst, M., R. de Hoogt, C. Hermans, M. Nellist, B. Janssen, S. Verhoef, D. Lindhout, A. van den Ouweland, D. Halley, J. Young, et al. 1997. Identification of the tuberous sclerosis gene TSC1 on chromosome 9q34. *Science.* 277:805–808.

van Slegtenhorst, M., M. Nellist, B. Nagelkerken, J. Cheadle, R. Snell, A. van den Ouweland, A. Reuser, J. Sampson, D. Halley, and P. van der Sluijs. 1998. Interaction between hamartin and tuberin, the TSC1 and TSC2 gene products. *Hum. Mol. Genet.* 7:1053–1057.

Walker, C., and J. Ginsler. 1992. Development of a quantitative in vitro transformation assay for kidney epithelial cells. *Carcinogenesis.* 13:25–32.

Wienecke, R., A. Konig, and J.E. DeClue. 1995. Identification of tuberin, the tuberous sclerosis-2 product. Tuberin possesses specific Rap1GAP activity. *J. Biol. Chem.* 270:16409–16414.

Yaffe, M.B. 2002. How do 14-3-3 proteins work? – Gatekeeper phosphorylation and the molecular anvil hypothesis. *FEBS Lett.* 513:53–57.

Yaffe, M.B., and A.E. Elia. 2001. Phosphoserine/threonine-binding domains. *Curr. Opin. Cell Biol.* 13:131–138.

Yaffe, M.B., G.G. Leparc, J. Lai, T. Obata, S. Volinia, and L.C. Cantley. 2001. A motif-based profile scanning approach for genome-wide prediction of signaling pathways. *Nat. Biotechnol.* 19:348–353.

Young, J., and S. Povey. 1998. The genetic basis of tuberous sclerosis. *Mol. Med. Today.* 4:313–319.

Zhang, Y., X. Gao, L.J. Saucedo, B. Ru, B.A. Edgar, and D. Pan. 2003. Rheb is a direct target of the tuberous sclerosis tumour suppressor proteins. *Nat. Cell Biol.* 5:578–581.